Ecological Indicators 183 (2026) 114659

Contents lists available at ScienceDirect

Ecological Indicators

journal homepage: www.elsevier.com/locate/ecolind

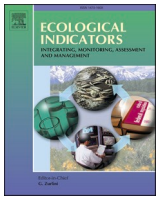

Linking species composition shifts from satellite time series to disturbance regimes and Lidar-derived structural and mortality indicators in boreal mixedwoods

José Riofrío [a,*], Nicholas C. Coops [a], Muhammad Waseem Ashiq [b], Alexis Achim [c]

[a] Department of Forest Resources Management, University of British Columbia, Vancouver, BC, Canada
[b] Science and Research Branch, Ontario Ministry of Natural Resources, Peterborough, ON, Canada
[c] Department of Wood and Forest Sciences, Université Laval, 2425 rue de la Terrasse, Québec, QC G1V 0A6, Canada

ARTICLE INFO

Keywords:
Species composition
Forest succession
Structural attributes
Mortality
Spruce budworm

ABSTRACT

Understanding species composition shifts in boreal mixedwoods forests is essential for anticipating forest succession pathways under changing disturbance regimes. Species composition transitions in boreal forests reflect complex successional processes influenced by interactions between disturbance regimes, structural dynamics, and species traits. In this study, we integrated satellite-derived annual species composition data with airborne laser scanning (ALS) structural metrics, spatially explicit mortality estimates and disturbance history to investigate composition transitions across ~288,000 ha of the Romeo Mallette Forest, Ontario. We focused on mid to late successional stages, identifying 27 species composition transitions and modeling their likelihood using extreme gradient boosting (XGBoost). From 2005 to 2018, 5% of the analyzed stands (~42,000 ha) predominantly transitioned from hardwood to coniferous or mixed compositions. Transition probabilities were strongly associated with ALS-derived gap metrics, mortality rates, and cumulative years of spruce budworm and Forest Tent Caterpillar defoliation, while traditional site factors had limited predictive value. Notably, the number of years affected by spruce budworm defoliation significantly increased the likelihood of transition in stands dominated by more susceptible species. The results advance our understanding of mid-late succession pathways and support the integration of remote sensing time series into forest monitoring frameworks, improving inventory accuracy, and guiding adaptive management under evolving disturbance regimes.

1. Introduction

Timely and accurate information on forest attributes is essential for establishing forest monitoring and management plans. Airborne laser scanning (ALS) provides detailed and accurate measurement of forest attributes like forest height, canopy cover, canopy gaps, standing volume and biomass with a high level of spatial detail and accuracy (Coops et al., 2021; White et al., 2017), making it increasingly valuable to develop Enhanced Forest Inventories (EFI) (Fassnacht et al., 2024; White et al., 2025). Complementary annual or sub-annual multispectral satellite data allows to periodically update EFI attributes enabling to monitor the status and change of forest resources and forecasting future attributes associated with specific management actions or changing environmental conditions (Coops et al., 2023).

However, forest inventories require additional forest attributes not readily estimated from typical ALS systems, which utilize single wavelengths and therefore have limited spectral differentiation on the return pulses. For example, species composition, which is used at the stand level to classify stands into different assemblages using estimations of species proportions by basal area, volume, canopy cover, or strata species occupancy (Little et al., 2024; Parton et al., 2006). Such assemblages then facilitate the development of various modeling products, for instance, yield/growth curves, silvicultural intensity regimes, and succession pathways, needed for forest management planning (Lennon et al., 2016; Penner and Pitt, 2019). As a result, manual interpretation of aerial imagery or the use of time-series of satellite imagery to generate species composition information often combined with climate and terrain information, is used to fill this important information gap.

When these datasets are combined, the level of spatial detail and accuracy can provide insights not only into the current structure and

* Corresponding author.
E-mail address: jose.riofriosalazar@ubc.ca (J. Riofrío).

https://doi.org/10.1016/j.ecolind.2026.114659
Received 27 August 2025; Received in revised form 12 January 2026; Accepted 20 January 2026
Available online 29 January 2026

composition of forest stands, but an also offer information from a variety of forest ecosystem processes. Forest succession, for example, represents changes in ecosystem functions, affecting wood supply, wildlife habitat provisioning, carbon storage, and other forest ecosystem services (Anyomi et al., 2022). Moreover, predicting stand forest succession remained a central challenge for scientists and foresters for over a century (Taylor et al., 2020); emerging different conceptual frameworks of vegetation succession, that for instance, hypothesized successional dynamics as a deterministic process though influenced by stochastic factors (Fenton and Bergeron, 2013; Taylor et al., 2020) or considering social and ecological interactions that operate at different spatial scales (Poorter et al., 2024). Following disturbance events, multiple succession pathways are possible depending on diverse mechanisms (Taylor and Chen, 2011) and complex interactions between the ecological properties of the regional species pool and the environmental conditions, disturbance regimes, and silvicultural prescriptions (Anyomi et al., 2022; Bergeron et al., 2014).

Principally, our understanding of forest succession has been driven by the use of successive measurements from permanent sample plots (Lennon et al., 2016; Taylor et al., 2020; Zhu et al., 2025). However, achieving a balanced representation of different environmental conditions, species abundance, and possible transitions requires long-term remeasurements over broad areas that are not always logistically or financially possible. Alternatively, multispectral satellite time series now provide consistent, long-term information for mapping tree species and stand structures and it is increasingly being applied to study the long-term temporal trends in vegetation composition and disturbance dynamics over large areas (Bonannella et al., 2024; Fassnacht et al., 2016; Hermosilla et al., 2024). Spatially detailed time series of species composition derived from remote sensing data facilitates the monitoring of changes in species over time and allows assessing the implications of changes on forest stability, management and ecosystem services (Wulder et al., 2024). Moreover, temporal consistency of species composition time series allows the analysis of the underlying process triggering composition shifts and successional dynamics (Gilić et al., 2023; Hermosilla et al., 2024). Furthermore, remotely sensed estimates of species composition, canopy structure, and mortality rates provide measurable and repeatable signals of forest condition and stability. These indicators are sensitive to disturbance regimes and successional processes and can be updated consistently through satellite time series.

Tree mortality or damage from non-stand replacing disturbances caused by insect infestation, drought, windthrow, competition, or silvicultural interventions alter the vertical structure, creating conditions for recruiting trees to establish and for remaining trees to access available resources, leading to changes in tree species composition over time (Bergeron et al., 2014; Brassard and Chen, 2010). Species compositional shifts at early and late stages might be driven primarily by tree growth and recruitment of individuals, while the relative contribution of mortality increases with the progression of ecological succession from middle to late stages (Nakadai and Suzuki, 2025). Thus, estimates of the standing basal area, volume, or biomass losses can provide insight into turnover; moreover, differences in mortality rates among species might also entail large differences in other ecosystem processes, such as species composition shifts and successional changes (Caspersen, 2004; Rees et al., 2001). In addition, interacting factors such as site conditions, species abundance, fire cycle, climate, and disturbances might result in a wide variation of forest composition changes (Anyomi et al., 2022).

In fact, recurrent eastern spruce budworm (*Choristoneura fumiferana* [Clem.]) and Forest tent caterpillar (*Malacosoma disstria* [Hbn.]) attacks are one of the main biological disturbances in Canada, producing annually moderate and severe tree defoliation events in Ontario since 2000 (National Forestry Database, 2025). Overall, stands affected by spruce budworm or Forest tent caterpillar (FTC) defoliation show changes in forest dynamics by reductions in tree vigour and canopy openness that produce volumetric timber losses and understory recruitment, causing forest structural and compositional changes (Chen and Popadiouk, 2002). Stability of species community and resistance and resilience patterns to spruce budworm outbreaks might vary widely depending on the dominant species (Hennigar et al., 2008) and composition and structure of the system (Sánchez-Pinillos et al., 2019; Trotto et al., 2024). In the case of FTC, variability in outbreak severity and duration creates a range of canopy structures altering regeneration patterns that however differ between mixed and deciduous dominated stands (Moulinier et al., 2013).

In this study, we examined relationships between disturbance regimes and stand-level structure dynamics, specifically mortality as detected from ALS tree canopy gaps, with available spatially explicit coverages of annual tree species composition, derived from Landsat imagery (Hermosilla et al., 2024). Our goal was to test whether a combination of remotely sensed stand structural and mortality indicators, together with spatially localized insect infestation information, helps explain ecologically plausible compositional transitions under conditions where the effects of insect outbreaks are expected to be subtle. To do so, we ask the following questions:

- What species transitions do we observe from annual species composition time series derived from Landsat imagery?
- Do the observed species transitions agree with the expected changes following successional transition rules in boreal environments?
- Do the different species composition changes relate to stand structure, mortality rate estimates, disturbance regime and site conditions?

Once answered, we identify and map areas where changes in species composition at the stand-level are likely to occur. The results provide not only insights for forest managers working in these and similar forest types on some likely transitions underway in their forest stands, but also provide a new methodology where advanced remote sensing methods, using data which is free and open, can provide informed insights into species-level changes in boreal and mixed forests more broadly.

2. Methods

2.1. Study area

The Romeo Mallette Forest (RMF) is a managed forest located in northern Ontario, Canada, within the Boreal Shield Ecozone (Fig. 1). Covering approximately 630,000 ha, 86% of this area is productive forest land, primarily used for timber production and fiber procurement. Management activities in RMF are guided by the Forest Management Plan based on a 10-year cycle (currently 2019–2029) following Ontario's Crown Forest Sustainability Act, which is publicly available at https://nrip.mnr.gov.on.ca/s/fmp-online?language=en_US. The managed productive forest land in RMF comprises 82% of regular production forest stands, 6% below regeneration status, 2% of protection forest, and 10% classified as recent disturbed stands. The managed stands are dominated by tree species such as black spruce (*Picea mariana* (Mill.) BSP), jack pine (*Pinus banksiana* Lamb.), trembling aspen (*Populus tremuloides* Michx), white spruce (*Picea glauca* (Moench) Voss), and paper birch (*Betula papyrifera* Marshall). Of these tree species, black spruce is the most prevalent in RMF, dominating 50% of the forest stands while only 8% of stands lack any proportion of black spruce. Management activities are scheduled and projected in Standard Forest Units (SFU) defined from tree species composition (Table 1), managed under the same silvicultural system, with about 70% of the harvested wood volume anticipated to come from black spruce, jack pine, and poplar-dominated stands. SFU's aggregate forest stands for management purposes based on tree species composition, succession following natural disturbances or silvicultural treatments (Little et al., 2024; Parton et al., 2006). Forest stands in the RMF are influenced by multiple disturbance agents, including wildfire, insect outbreaks, harvesting, and silvicultural activities. Resulting in diverse stand ages and development stages, with

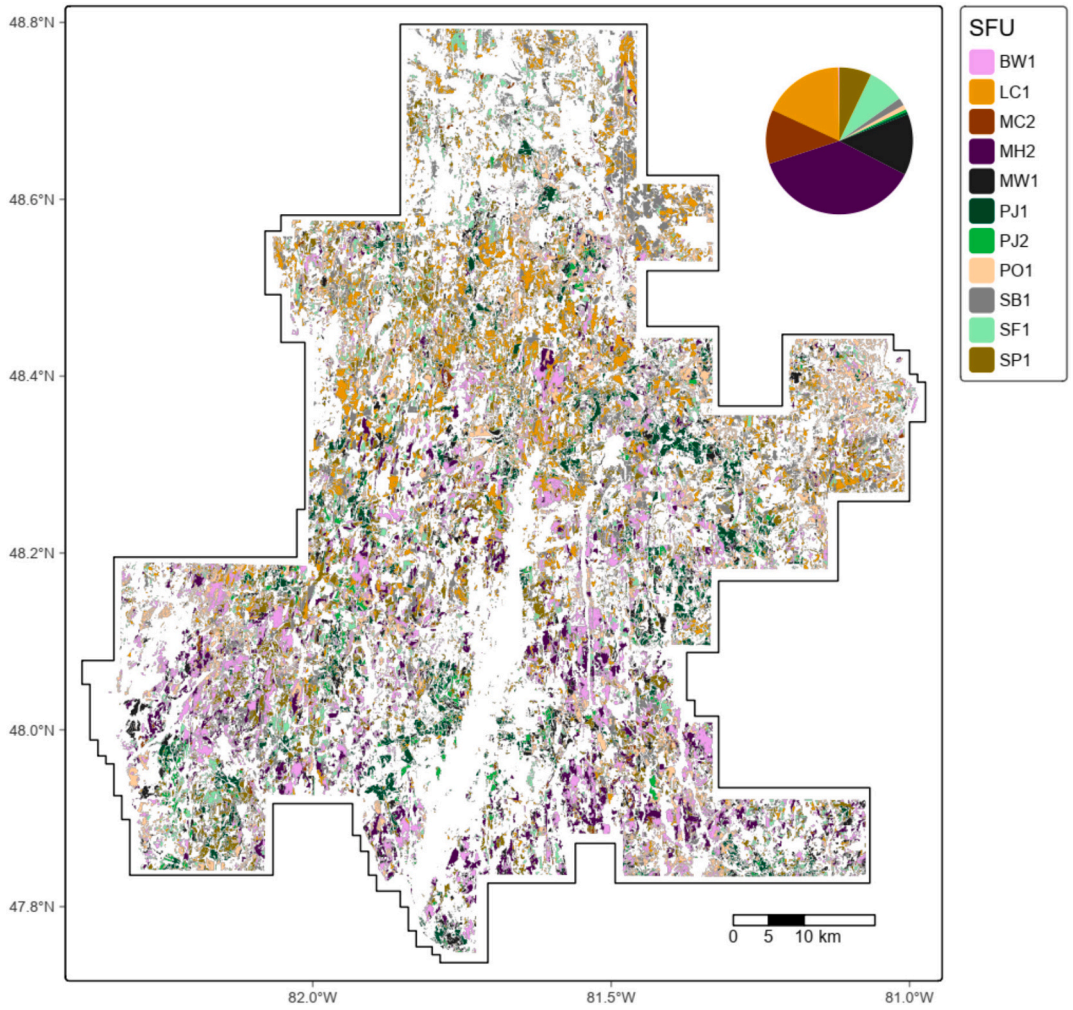

Fig. 1. Standard Forest Unit (SFU) classes in the Romeo Mallette Forest were defined from Landsat species composition maps with relative proportions of SFU in the study area. SFU's abbreviations in Table 1.

considerable managed forest area (38%) in operable age classes (60–100). The terrain varies from flat and water-saturated in the north to moderately rolling and better drained in the south, with elevations between 280 and 450 m. The forest experiences long, cold winters and short, warm summers, with average temperatures ranging from −16.8 °C to 17.5 °C.

2.2. Data

2.2.1. Species composition time series

We used the satellite-derived time series of the major dominant tree species of Canada's forested ecosystems developed by Hermosilla et al. (2024). The national-level annual tree species maps from 1984 to 2022 were calibrated based on Canada's National Forest Inventory (Gillis et al., 2005) using regional Random Forest classification models. Species composition time series were generated using predictor variables derived from Landsat surface reflectance best-available-pixel image composites, combined with geographic, climate, phenological, and topographic data (Hermosilla et al., 2022). The annual dominant tree species classification presented by Hermosilla et al. (2024) showed an overall accuracy of 86.1% ± 0.14% (95% confidence interval), and predicted both the leading tree species as well as the likelihood of class membership to each of the targeted 37 species at 30 m resolution (Hermosilla et al., 2024). The membership likelihoods provide the confidence associated with the presence of tree species in addition to those classified as leading, allowing for defining the proportion of each species and assigning tree species assemblages at the stand level (Hermosilla et al., 2022; Sales et al., 2022; Wulder et al., 2024).

2.2.2. Forest resources inventory

A polygon-based Forest Resources Inventory (FRI) available for RMF was initially established with manual photo-interpretation of multi-spectral aerial imagery acquired in 2005. FRI polygons reflect information about tree cover, composition, successional stage, and silvicultural interventions. About 20% of the stands initially established were updated using new aerial photographs or field-based surveys regularly until 2014 to account for harvesting, natural depletion, silvicultural treatments, regeneration, or changes in stand development stages. Our analysis focused exclusively on polygons of productive forested type with a minimum area of 10,000 m^2.

We extracted stand age and site conditions descriptors for each stand from the FRI attributes. Stand age was calculated for each stand using the origin year. FRI also included moisture regime (MR), nutrients regime (NR) and site class (SC) as indicators for site conditions. MR and NR are relative rankings of substrate moisture and nutrient supply throughout the growing season, estimated based on variations in texture, pore pattern, substrate depth, topographical position, and drainage (MNR, 2021). In order to simplify the interpretation of the results, we summarized the MR levels into four classes, i.e., dry, fresh, moist and wet; and the NR levels into three classes, poor, medium and rich. SC is considered a proxy of the site quality of the stands and is defined using species-specific height and age growth curves for the

Table 1
Criteria of species proportion composition to assign Standard Forest Units (SFU) classes used in the RMF Forest Management Plan 2019–2029 (MNR, 2018).

Standard forest units (SFU)	Species proportion criteria	Description
White and red pine (PRW)	Red pine ≥ 70 OR (White pine + Red pine + White spruce ≥ 40 AND White pine≥ 30) OR White pine + Red pine ≥ 40	Stands are dominated by red pine or red pine-white pine mixture growing on a variety of soil types, from dry to moist sites and sandy to silty soils. Stands are an uncommon forest unit in the boreal northeast.
Tolerant-lowland Hardwood (OH1)	Black ash + White elm + Balsam poplar ≥ 30 OR Black ash + Elm + Balsam poplar + Sugar maple + Yellow birch + Red maple ≥ 30	Stands containing primarily self-replacing, tolerant hardwood species on upland sites with sandy to coarse loamy soils of morainal origin.
Spruce bog (BOG)	Black spruce + American larch ≥ 70 AND White pine = 0	Stands are dominated by low-productivity black spruce and larch. Stands principally for biodiversity and wildlife habitat purposes related to sustainable forest management planning.
Black spruce (SB1)	Black spruce ≥ 70 AND (Sugar maple + Red maple + Yellow birch + Red pine) =0 AND (Jack pine + White Pine) ≤10	Stands dominated by black spruce growing on wet, deep organic soils and on moist, peaty-phase mineral soils in lower slope positions. These stands can be of fire origin and will self-replace.
Jack pine (PJ1)	(Jack pine ≥ 70 AND (Trembling aspen + Largetooth aspen + White birch + Silver maple` + Black ash + Balsam poplar + Red maple + Elm + Yellow birch) ≤20	Stands are dominated by jack pine growing on dry to fresh, sandy to coarse loamy soils of glaciofluvial origin. These stands are of fire origin. Stands 120 years and older on dry sites where the pine component has declined to as low as 50% are still included in this SFU.
Lowland Conifer (LC1)	(Eastern white cedar + American larch + Black spruce) ≥70 AND (Sugar maple + Red maple + Yellow birch + Red pine) =0 AND (White Pine + Jack pine) ≤10	Mixed stands of black spruce, larch, and (or) eastern white-cedar occupy wet, moderately deep organic soils associated with drainage ways or the toe of slopes where telluric water augments the on-site nutrient pool. These stands rarely burn and will self-replace. This SFU can also include stands with white birch on organic soils.
Pine-Spruce (PJ2)	((Jack pine + Black spruce + Red pine) ≥70 OR (Jack pine≥ 50 AND (Jack pine + Black spruce + Balsam fir + White spruce + Eastern hemlock + White Pine + Red pine + Eastern white cedar + American larch) ≥70)) AND (Jack Pine ≥ Black Spruce)	Mixed stands of jack pine and black spruce growing on dry to moist, sandy to coarse loamy soils of glaciofluvial origin. These stands are of fire origin or will develop with time from PJ1. Jack pine stands with an important balsam fir component are included in this SFU.
Spruce-Pine (SP1)	(Black spruce + White spruce + Balsam fir + Eastern white cedar + American larch + White pine + Jack pine + Red pine + Eastern hemlock) ≥70 AND ((Balsam Fir + Eastern white cedar + White pine + American larch + White spruce + Eastern hemlock) ≤20 OR (Jack Pine) ≥30)	Stands are upland black spruce-dominated conifer stands on fresh to moist mineral soils of all textures. They can include almost pure black spruce stands with very little or no jack pine. These stands are of fire origin or will develop through succession from other forest types.
Spruce-Fir (SF1)	(Black spruce + White spruce + Balsam fir + Eastern white cedar + American larch + White pine + Jack pine + Red pine) ≥70	Mixed conifer stands of white spruce, balsam fir, black spruce, and eastern white cedar growing on fresh to moist mineral soils of all textures. This SFU develops primarily from succession and rarely from fire origin. Highly productive stands are often found on lower slope positions associated with telluric seepage.
Poplar (PO1)	(Trembling aspen + Balsam poplar + White birch + Sugar maple + Black ash + Red maple + Yellow birch + Elm) ≥70 AND (Trembling aspen + Largetooth aspen + Balsam poplar) ≥50	Hardwood stands dominated by trembling aspen. They typically occur on fresh to moist, loamy to clayey soils. These stands are primarily of fire origin.
Birch-Poplar (BW1)	(Trembling aspen + Largetooth aspen + Balsam poplar + White birch + Sugar maple + Black ash + Red maple + Yellow birch + Elm) ≥70	Hardwood stands dominated by white birch. They occupy some of the same sites that PO stands occupy, as well as somewhat drier and coarser-textured soils. They can be of fire origin or develop through succession from other forest conditions.
Mixedwoods (MW1)	(Jack pine + Red Pine) ≥20 OR (Balsam fir ≤20 AND White spruce ≤20 AND Eastern white cedar ≤20)	Mixed conifer-deciduous stands comprising trembling aspen, white birch, jack pine, and black and white spruce. They occur on dry to moist, sandy to coarse loamy soils. These stands can be fire origin or develop through succession. Stands that have undergone succession may lack jack pine but will have <20% late successional species such as balsam fir, white spruce, and eastern white-cedar in the canopy.
Mixed Hardwood (MH2)	(Trembling aspen + Largetooth aspen + White birch + Sugar maple + Yellow birch + Red maple + Black ash + Elm + Balsam poplar) ≥50	Stands are mixed conifer-deciduous, comprising largely trembling aspen, white birch (>50%). Black and white spruce, balsam fir, or eastern white-cedar represent less than 50%. They occupy fresh to moist, medium loamy to clayey soils. These stands most often develop through succession from other SFUs.
Mixed Conifers (MC2)	(Black spruce + White spruce + Balsam fir + Eastern white cedar + American larch + White pine + Jack pine + Red pine) >50 AND all remaining stands.	Mixed conifer stands comprising largely black and white spruce, balsam fir, and eastern white-cedar. They occupy fresh to moist, medium loamy to clayey soils. These stands most often develop through succession from other SFUs

dominant tree species (MNR, 2009). We removed stands with records of recent silviculture interventions, for instance, commercial thinning or spacing treatment. We also excluded stands with exposed bedrock or minimal soil depth, where forest regeneration and growth would be constrained due to poor growing conditions.

2.2.3. Mortality rate model

In the absence of stand-replacing disturbances (specifically wildfires and harvesting), tree mortality or damage from non-stand-replacing disturbances (mainly caused by insect infestation, drought, wind-throw, competition, or silvicultural interventions) leads to changes in

forest structure and tree species composition over time (Bergeron et al., 2014; Brassard and Chen, 2010). Tree mortality from non-stand-replacing disturbances creates canopy gaps and changes in the vertical structure of the stand (McCarthy, 2001; Yamamoto, 2000). Riofrío et al. (2025) demonstrated that ALS data can be used to estimate stand-level mortality over large areas through the characterization of canopy gaps, vertical and horizontal structural complexity.

In this study we used the mortality rate model developed by Riofrío et al. (2025) that provides spatially explicit estimates of mortality probability and mortality rates at 20 m resolution across forest types and structural attributes over the RMF. The model relies on data from repeated measurements of permanent sample plots and ALS point cloud data and requires stand-level factors, such as stand age and species composition and ALS-derived metrics related to canopy structure and canopy gaps as predictors. The model was calibrated using mortality rate observations of permanent sample plots, showing a RMSE of 0.0107 and model efficiency of 0.373 and revealed the spatial variation of the expected mortality rates across boreal mixedwood forests.

There are three key considerations regarding the mortality model application in our analysis. First, the model was designed to inform stand-level mortality rates attributable to non-stand-replacing disturbances. The model was fit considering only permanent sample plots with a mortality rate lower than 0.1, avoiding mortality events that might be triggered by stand-replacing disturbances. Second, the model estimates the proportion of basal area loss (mortality rate) between concurrent plot measurements. Basal area loss may be a better indicator of disturbance severity (Hart and Kleinman, 2018) for compositional shifts at middle to late stand development stages (Nakadai and Suzuki, 2025), because after the stem exclusion phase, as the stand matures, compositional shifts based on dominance (i.e., basal area) are mainly influenced by the mortality of large trees rather than recruitment (Nakadai and Suzuki, 2025). Finally, because the mortality rate model was calibrated using plot measurements between 2004 and 2020, the target period in this study was selected to match the interval of the mortality rate predictions. During this period, we calculated the mean (MorR_mean) and standard deviation (MorR_sd) mortality rate for each stand selected in the analysis.

2.2.4. ALS-derived variables

ALS data was acquired in June–July 2018 under leaf-on conditions using a Leica SPL100 single photon LiDAR (SPL) sensor operating at a green wavelength ($\lambda = 532$ nm). The SPL system emitted pulses in a 10 $\times$ 10 beamlet array and was flown at an average altitude of 3800 m above ground level with a nominal speed of 350 km/h along parallel flight lines with 50% overlap. Data acquisition adhered to the Ontario Specification for LiDAR Acquisition (MNR, 2016), yielding a vertical accuracy class of 2.6 cm and a reported vertical RMSE of 5.1 cm. Post-processing by the data provider included noise filtering, georeferencing, and classification based on (Gluckman, 2016), resulting in an average point cloud density of 40 points/m^2. Point clouds were normalized to above-ground height using a triangulated irregular network of ground returns.

Normalized ALS data was used to derive vegetation structure metrics on a 30 $\times$ 30 m grid aligned with the Landsat-based species composition time-series. ALS data processing was conducted using the *lidR* R package (Roussel et al., 2020). The 99th percentile height of first returns (p99) was calculated, likewise the mean (p99_mean) and standard deviation (p99_sd) of p99 were computed by each delineated polygon (i.e., stand) included in the analysis. Canopy gaps were identified from a 0.5 m resolution canopy height model (CHM) generated using the pit-free algorithm (Khosravipour et al., 2014). Gaps were delineated using the *ForestGapR* package (Silva et al., 2019) with a fixed height threshold of $<$3 m, following established thresholds for boreal and temperate forests in Canada (Goodbody et al., 2020; White et al., 2018). Only contiguous gaps between 4 m^2 and 10,000 m^2 were retained. To exclude anthropogenic disturbances such as forestry roads, gaps were filtered using a shape index (Patton, 1975), calculated as $\left(p/(2 \times \pi \times a)^{0.5}\right)$, where p is perimeter and a is area of a given gap. Gaps with a shape index $>$3 and area $>$ 100 m^2 were excluded to remove long, narrow, likely non-regenerating gaps. Finally, the proportional gap area (GapProp) by stand was also computed from the delineated canopy gaps.

2.2.5. Disturbances caused by insect damage events

Data on non-stand-replacing disturbances due to insect damage were gathered from the available disturbance layers produced by the Ontario Ministry of Natural Resources (MNR). Mapped events of forest insect damaging trees by defoliation, foliage mining and wood boring are produced on an annual basis, providing georeferenced layers publicly available online (https://geohub.lio.gov.on.ca/) (MNR, 2024). We calculated the cumulative number of years of moderate to severe defoliation or insect damage events between 2000 and 2020, computed at 30x30m resolution for the main insect outbreaks: eastern spruce budworm (*Choristoneura fumiferana* [Clem.]) and Forest Tent Caterpillar (*Malacosoma disstria* [Hbn.]). Fig. 2 indicates a relatively mild outbreak of spruce budworm in the north of RMF, and only 1–3 years of defoliation in the south. Similarly for FTC, there was some lengthy defoliation on the far eastern edge of the RMF.

Given the limited and spatially variable spruce budworm and Forest Tent Caterpillar activity during 2000–2020, we anticipated that any insect-driven signals would be subtle. Our goal was therefore not to detect major outbreak impacts—which are unlikely in this context—but to test whether remotely sensed indicators from stand structural and mortality estimates together with subtle insect-related effects help explain ecologically meaningful species compositional transitions.

2.3. Analysis approach

2.3.1. Building species composition transitions

In this study, we use class membership likelihood ranks derived from the Random Forest tree species classification (Hermosilla et al., 2024) to assign standard forest units (SFU) at the stand-level (i.e., delineated polygons available in the FRI). We calculated the relative frequency of the class membership likelihood values from the species present in each stand by averaging the class membership probability estimates of each class over all pixels (Sales et al., 2022; Wulder et al., 2024). We included only species with a relative presence in the stand greater than 2.5%. Additionally, to prevent the noise from random probability assignments in the classification algorithm and to ensure that tree species with low probabilities were not included, pixels with class membership likelihood values of $\leq$ 5% were excluded (Wulder et al., 2024). Then, class membership percentages by species were used to assign each polygon to SFU following the classification system implemented in the forest management plan for the Romeo Malette Forest (MNR, 2018). This classification system uses a modified version of the classification criteria from Parton et al. (2006). Table 1 depicts the SFU definition based on species composition proportion. SFUs in Table 1 are ordered according to the classification criteria algorithm (Little et al., 2024; MNR, 2018).

From the total available stand inventory data (43,806 productive forest stands), we selected 28,493 stands covering 287,975 ha that fit the criteria as follows (Fig. 1). First, as we are interested in changes in species composition due to non-stand-replacing disturbances in stands at middle to late development stages, stands younger than 30 years were excluded to remove early stand succession pathways following stand-replacing disturbances (i.e., harvesting). In addition, because some SFU successional transitions are unlikely to occur in the absence of stand-replacing disturbances or they are too rare, we only considered the SFU empirical succession rules implemented in the current forest management plan of the study area (Lennon et al., 2016). Thus, only possible SFU changes (Fig. 3) were included in the analysis to reduce the unnecessary dimensions of the SFU transitions in the classification model. Our analysis was focused on the SFU transitions between 2005 and 2018

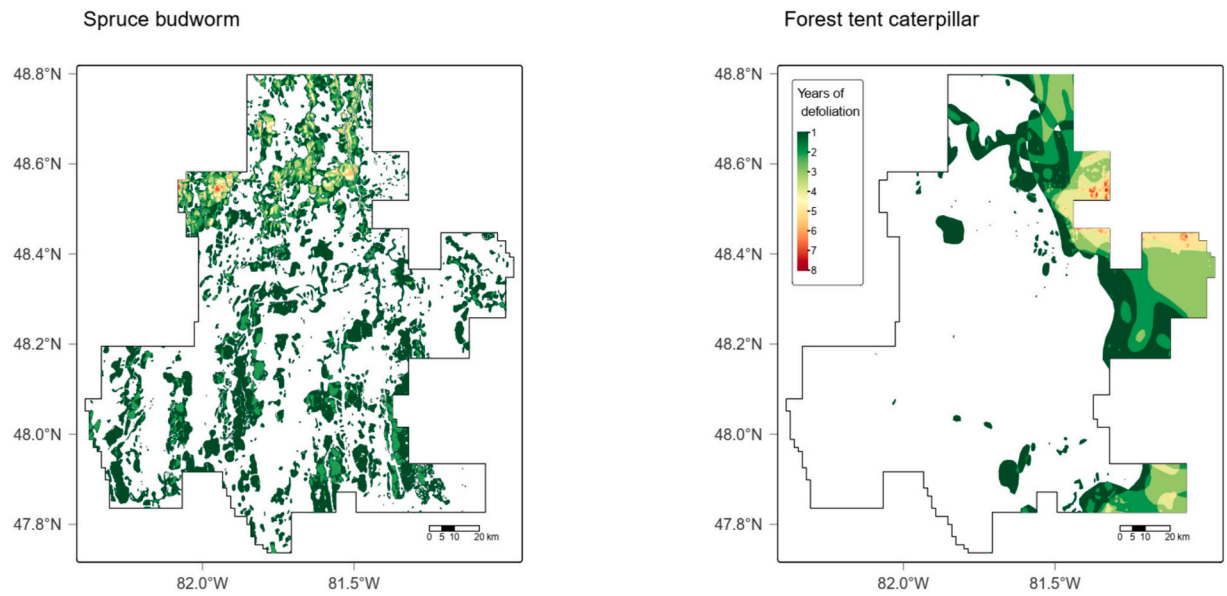

Fig. 2. Total number of years of moderate-to-severe defoliation, 2000–2020, in the RMF during the most recent eastern spruce budworm and Forest Tent Caterpillar outbreaks, data source MNR (2024).

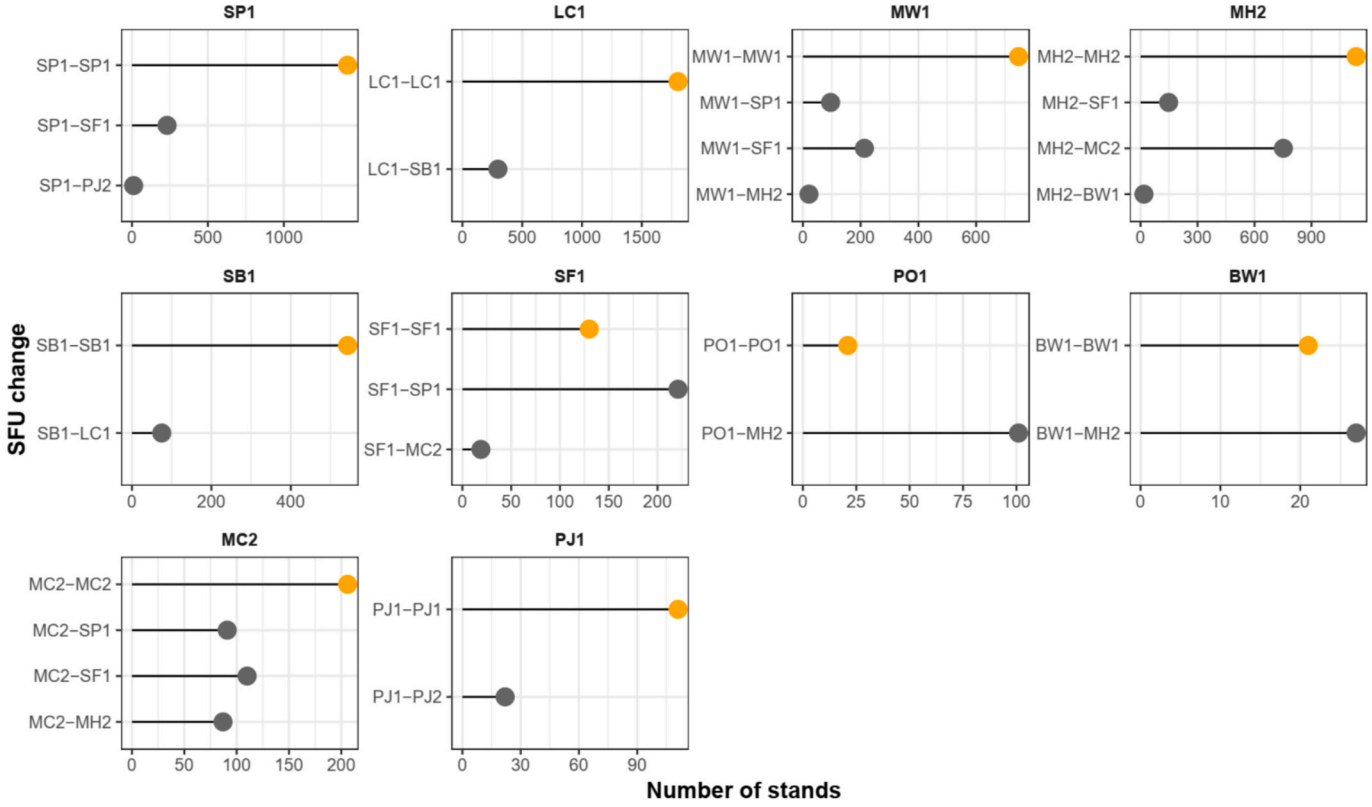

Fig. 3. Standard Forest Units (SFU) transitions between 2005 and 2018, solid grey dots are the number stand transitioning SFU class while orange are stand that reminded stable. The X axis shows the number of stands by SFU transition. SFU's abbreviations in Table 1.

to match the calibration period of the mortality rate model. Finally, to improve the consistency and reduce the uncertainty of the likelihood of species class membership from the model, we selected stands that maintained the same SFU class four years before or after the analysis period (2005–2018). Finally, we check the Landsat-derived SFU classification to the corresponding FRI photo-interpreted SFUs matching each stand to the year in which it was last updated in the FRI (Fig. S1).

2.3.2. *Modeling species composition transitions*

In order to determine whether species composition transitions were predictable from a set of explanatory variables (Table 2), we used the extreme gradient boosting algorithm (XGBoost) (Chen and Guestrin, 2016). XGBoost is a scalable machine learning method for tree boosting regression and classification based on an iterative process that improves model performance by adding trees to reduce a loss function (Friedman, 2001; Natekin and Knoll, 2013). This machine learning approach can

Table 2
Description of explanatory variables used in the XGBoost species composition transitions models.

Variable	Description	Unit	Range (mean)
AGE	Stand age	Continuous (yr)	43–200 (85)
MRs	Moisture regime	Ordinal	dry, fresh, moist, wet
NR	Nutrients regime	Ordinal	rich, medium, poor
Site_class	site class indicator	Ordinal	best, better, good, poor, very poor
MorR_mean	Mean stand mortality rate	Continuous (proportion yr^{-1})	0–0.05 (0.07)
MorR_sd	Standard deviation of mortality rate within the stand	Continuous (proportion yr^{-1})	0–0.02 (0.004)
GapProp	Gap proportion area of the stand	Continuous (proportion)	0–0.2 (0.06)
p99_mean	Mean stand height	Continuous (m)	6.5–27.9 (18.1)
p99_sd	Standard deviation of height within the stand	Continuous (m)	0.7–9.3 (2.7)
SpBud_max	Total number of years of moderate-to-severe defoliation due to spruce budworm	Continuous (yr)	0–4 (0.2)
Tent_max	Total number of years of moderate-to-severe defoliation due to tent caterpillar	Continuous (yr)	0–8 (0.5)

accommodate diverse data distributions and deal with non-normality and heteroscedasticity, common issues in ecological data. Tree boosting regression analysis is suitable for handling complex, nonlinear relationships, including interactions in ecological data and has been used to model multiple succession pathways following disturbances in stands at different development stages (Liu and Yang, 2014; Taylor et al., 2020; Vidal-Macua et al., 2017).

We fit independent models for each initial SFU class. XGBoost models were fitted using the SFU's transition classes identified from the satellite-derived species composition as a categorical response variable. We used a Bernoulli or multinomial response distributions for SFU with two or more than two SFU transition classes, respectively. To ensure unbiased model performance estimates, the data was split into 70% training and 30% test sets, with hyperparameter tuning conducted via 10-fold cross-validation on the training set and "*mlogloss*" as the evaluation metric for hyperparameter combinations in each model construction. Given the large number of possible combinations of hyperparameters in the XGBoost model, we use the learning curve combined with the Grid-Search method for model tuning to determine the optimal combination of hyperparameters, including eta (0.1–1), max.depth (2–6), subsample (0.1–1), bytrees (0.4–1), nrounds (50–200), and learning_rate (0.01–1). Optimal settings were based on changes in Area Under the Curve (AUC) from cross-validation, with a change >0.1 considered significant (Ferri et al., 2009). In addition, because all the SFU change classes are not equally represented across the training data (Fig. 3), this is expected to result in poorer model performance for rarer SFU transition classes and better performance for more common ones. We balanced the samples in each SFU change class by reducing the number of samples in the larger classes (downsampling).

XGBoost models were developed in R using the 'caret' package (Kuhn, 2015) for hyperparameter tuning and the *xgboost* package (Chen and Guestrin, 2016) for model fitting. Model interpretation involved examining the relative influence of variables and plotting partial dependency plots (PDPs) (Greenwell et al., 2019). Variable relative importance was scaled between 1 and 100 (the most important explanatory variable) and calculated based on the number of times a predictor was selected for splitting an individual tree and the improvement to the model as a result of each split (Friedman and Meulman, 2003; Hastie et al., 2009). We also calculated the variable importance separately for each SFU change class of the multinomial models by summing model improvement at each split for each variable and class (Hastie et al., 2009; Taylor et al., 2020). Thus, we were able to assess which variables contributed the most to each SFU change class as well as to the overall models. PDPs illustrate the marginal effects of one predictor variable over the response outcome while other variables are kept constant. PDPs provide a useful basis for interpretation, accounting for interactions, and capturing the non-linear, non-monotonic relationships between variables and response probabilities (Greenwell, 2017). We only showed partial dependency plots for the five variables that contributed the most in each overall SFU model according to their scaled relative influence.

Finally, the accuracy of the models for each SFU and SFU transition class was evaluated using the test dataset. We calculated the overall accuracy (OA) and No Information Rate (NIR) across all SFU models. The OA is a global measure of accuracy that indicates the proportion of observations that were correctly classified. The NIR is the proportion of stands correctly classified in the largest SFU change class, indicating the accuracy of the model if only the largest class is predicted. In addition, we calculated the recall (producer's accuracy – PA), precision (user's accuracy - UA), and the F-score for each SFU change class. PA represents the proportion of correctly identified SFU change classes to all the possible transition pathways, while UA measures the proportion of correctly identified SFU classes among the predicted SFU change classes. The F-score combines recall and precision, providing a balanced metric that penalizes discrepancies between recall and precision and ensures robust performance evaluation.

3. Results

The satellite-derived species composition layers allowed to identify 27 different composition transitions in stands at middle to late development stages, ranging from 2 to 4 different classes by initial SFU. Regardless of the stands that maintained the same species composition, the most common transition was MH2-MC2 (Hardwoods leading stands to conifer mixedwoods), representing 14% of the total stands analyzed, followed by SF1-SP1 (spruce-fir to spruce-pine dominant stands) at 4%. On the other hand, the less represented (< 30 stands) composition transitions in the dataset were SF1-MC2 (18 stands) and MH2-BW1 (16 stands) (Fig. 3).

3.1. XGBoosted regression tree performance

The accuracy of the models over the test data for each SFU is presented in Table 3. Models yielded OAs ranging from the lowest 0.37 for SFU transitioning from mixed hardwoods (MH2) to the highest of 0.83 for jack pine-dominated stands (PJ1), indicating a moderate performance for all the models. Most of the models showed a greater NIR in comparison to OA, except the model for poplar-birch stands (BW1). Furthermore, we also evaluated the performance of each SFU transition class using the recall, precision and F-score indicators (Table 3). The models with only two possible SFU changes showed better performance in comparison to the multinomial models (i.e., more than 2 possible SFU transitions), showing recall and precision values greater than 0.4. When multiple SFU transition pathways were modeled, the ability of the models to predict the correct class decreased as the model complexity increased. We also note that the less represented SFU change classes in the testing data to evaluate multinomial models showed the lower F-score values, for instance, the transitions SF1-MC2 and MH2-BW1.

3.2. Relative importance of variables

The overall scaled variable importance from each SFU model is presented in Fig. 4. The best-ranked variables in relative importance

Table 3
Performance diagnostics of XGBoost models over test data for each SFU class.

SFU	OA	NIR	SFU transition	Recall (PA)	Precision (UA)	F-score
BW1	0.67	0.58	BW1-BW1	0.40	0.67	0.50
			BW1-MH2	0.86	0.67	0.75
LC1	0.72	0.88	LC1-LC1	0.74	0.94	0.83
			LC1-SB1	0.66	0.26	0.37
MC2	0.42	0.42	MC2-MC2	0.42	0.55	0.47
			MC2-MH2	0.26	0.18	0.21
			MC2-SF1	0.14	0.16	0.15
			MC2-SP1	0.87	0.70	0.78
MH2	0.37	0.56	MH2-MH2	0.33	0.62	0.43
			MH2-BW1	0.25	0.01	0.02
			MH2-MC2	0.40	0.42	0.41
			MH2-SF1	0.47	0.17	0.25
MW1	0.44	0.70	MW1-MW1	0.46	0.79	0.58
			MW1-MH2	0.60	0.06	0.11
			MW1-SF1	0.29	0.19	0.23
			MW1-SP1	0.60	0.39	0.48
PJ1	0.83	0.81	PJ1-PJ1	0.88	0.92	0.90
			PJ1-PJ2	0.67	0.57	0.61
PO1	0.44	0.85	PO1-PO1	0.80	0.18	0.29
			PO1-MH2	0.38	0.92	0.57
SB1	0.66	0.87	SB1-SB1	0.63	0.97	0.76
			SB1-LC1	0.86	0.26	0.40
SF1	0.47	0.65	SF1-SF1	0.26	0.37	0.31
			SF1-MC2	0.67	0.07	0.13
			SF1-SP1	0.56	0.87	0.68
SP1	0.60	0.81	SP1-SP1	0.59	0.87	0.70
			SP1-SF1	0.61	0.26	0.36

OA: overall accuracy, NIR: no information rate. SFU's abbreviations in Table 1.

values varied across all models. However, the most common variables showing the higher variable importance were the stand proportion of gap area (GapProp), mean (p99_mean) and standard deviation (p99_sd) of stand height, the mean (MorR_mean) and standard deviation (MorR_sd) of mortality rate of the stand and the number of years with defoliation events by spruce budworm (SpBud_max). Overall, the models depicted two to five variables with scaled importance values greater than 50%. One single variable showed considerably higher importance values than the other predictor variables (<25%) only in the models for lowland conifer (LC1) and jack pine stands (PJ1). It is worth noting that, stand age and site condition variables (MRs, NR and Site class) ranked low overall.

In the five SFU transition models predicting a multinomial response (MC2, MH2, MW1, SF1 and SP1), in addition to the overall variable influence, we calculated separately the scaled variable influence for the multiple pathways of species composition change (Fig. S2). We found that for some models, the importance values for the most relevant variables (>50%) changed among the different SFU transitions despite the same variables being ranked in the top five positions. For instance, the SFU transition models for mixed conifer stands (MC2) and spruce-fir (SF1) stands are mainly influenced by gap proportion, mortality rate and stand height. Conversely, the overall ranking for the transition models for mixed hardwoods and mixedwoods varied widely among some SFU transition classes. This is true for the transitions MH2-MC2 and MW1-MH2, where the most important variable in the overall ranking had a markedly lower importance. The relative importance of the variables related to site conditions (nutrient -NR and moisture-MR regime) remained lower than 20% for most SFU change classes.

3.3. Mapping the probability of species composition change

Mapping the probability of species composition change at the stand level was produced by the composite of the SFU XGBoost models (Fig. 5). Overall, the models predicted that 5% (3538 stands covering ~42,000 ha) of the selected stands are likely to change species composition between 2005 and 2018. The proportional area predicted to show some transition varied among SFU classes; the greater relative proportion of stands changing class was for stands initially classified as mixed conifers (71%) and mixed hardwoods (69%), and the lowest for birch-poplar dominated stands (1%) (Fig. S3). Although stands showing a higher probability of species composition change were scattered throughout the RMF, mixed conifer and hardwood stands showing species changes were predominantly located in the southern area of the RMF (inset B, Fig. 5). In the central and northern areas, mostly stands dominated by black spruce, fir and pine species were less prone to species composition changes (inset A, Fig. 5).

3.4. Explanatory variables for SFU transitions

In order to synthesize the results, Appendix 1 (Figs. S4 to S8) displays the partial dependence plots (PDP) for the five most important variables in each SFU model. In addition, to facilitate the comparison of the relationship between the SFU change classes and explanatory variables, the SFUs were grouped into 4 sets according to the dominant species. Thus, black spruce dominant stands (Fig. S4), jack pine dominant stands (Fig. S5), spruce-fir-pine codominant stands (Fig. S6), conifer and hardwood mixedwood stands (Fig. S7), and deciduous dominated stands (Fig. S8). In general, models with only two possible transition pathways showed clearer threshold values across variables distinguishing the probability transitions than the multinomial response transition models. However, even in a more complex model with multiple SFU change pathways, variables like mortality rate and canopy height showed marked tipping points defining the probability of SFU transitioning from one class to another; therefore, we emphasize the role of these variables when types of transitions are compared.

As shown in Fig. 6, partial dependence plots demonstrate the influence of spruce budworm defoliation outbreaks on the likelihood of SFU transition pathways, revealing that the probability of transitioning from spruce-fir (SF1) or mixedwoods (MW1) to spruce-pine (SP1) increases notably after repeated defoliation events. The effect is particularly pronounced beyond a threshold of 2–3 years of cumulative defoliation, supporting the idea that repeated insect disturbances are a major driver of compositional change in susceptible forest types. Forest tent caterpillar (FTC) activity was more temporally persistent (4–7 years) and spatially concentrated in the eastern RMF than the mild and short (1–3 years) spruce budworm defoliation observed during 2000–2020 (Fig. 2). The partial dependence curve for FTC shows a less intense and non-linear effect in transition probability at higher defoliation intensities for trembling aspen dominated stands (PO1).

4. Discussion

Information on how species assemblages are changing over time can be difficult to attain on a spatially explicit basis. The recent availability of high-quality time series of surface reflectance information derived from satellite remote sensing is providing a previously unavailable source of information which can be used to derive tree species information over space and time (Hermosilla et al., 2024). The availability of annual dominant species spatial estimates across Canada has enabled the analysis of successional dynamics to be undertaken and demonstrates the capacity of how these types of datasets can be used when they

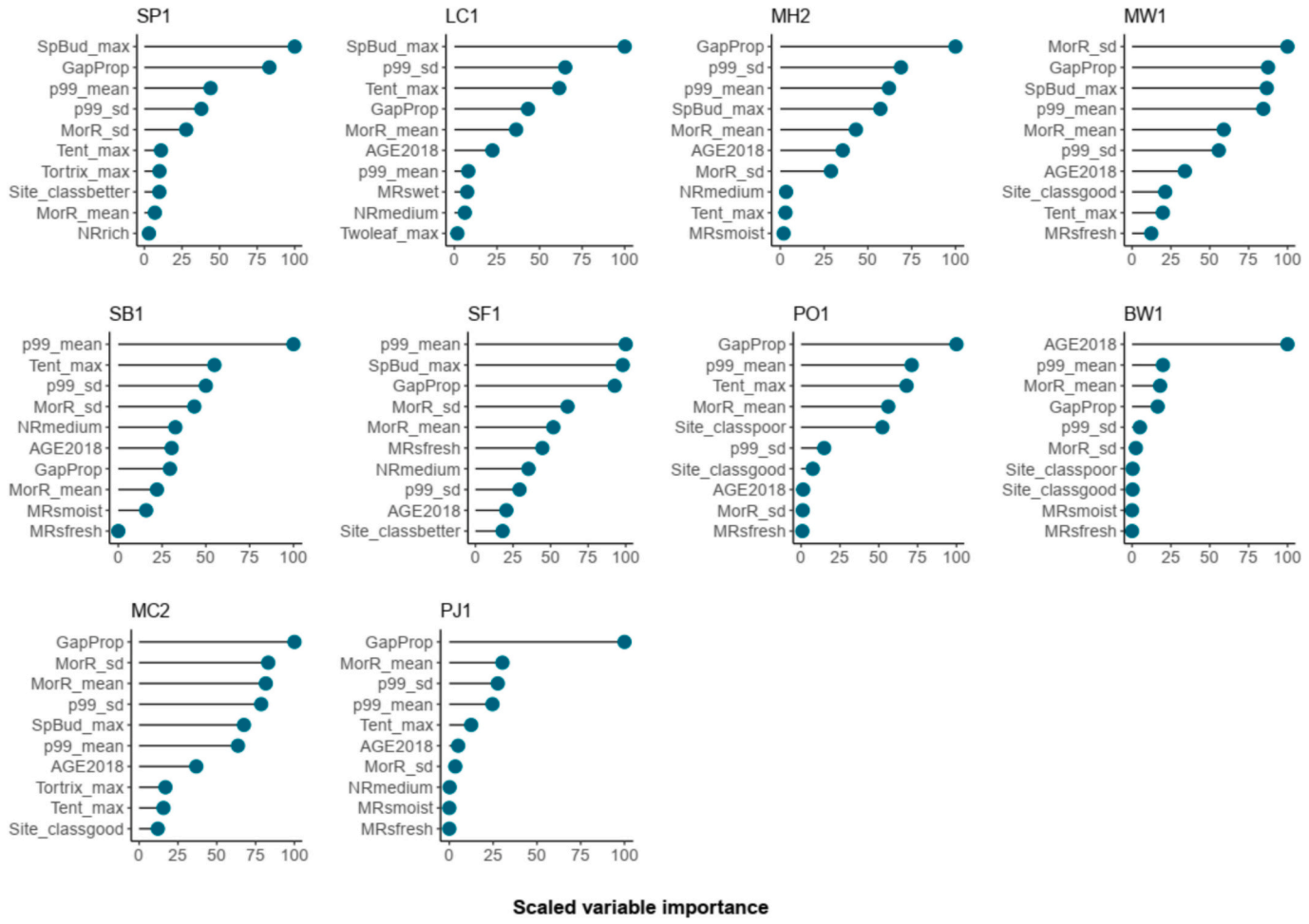

Fig. 4. Scaled variable importance in the final XGBoost models for each SFU. Refer to Table 1 for SFU class and Table 2 for all variable abbreviations.

made available. We acknowledge, however, that the satellite data record is relatively short compared to tree species successional pathways, with satellite data only available since the mid-1970s. As a result, we are only able to observe relatively subtle changes in species composition over this 40–50-year time window. Obviously, mortality and succession timelines are significantly longer (Taylor and Chen, 2011; Zhu et al., 2025) than the relatively short period of time in our analysis, which corresponds to the years for which morality estimates and derived ALS-structural attributes are consistently available.

The relatively short period explains why stand age was ranked among the less important variables in the succession models. This result agrees with Zhu et al. (2025), the authors demonstrated that stand age is a weak predictor of species compositional changes using repeated standard forest mensuration data. As indicated throughout this analysis, the age of the stand is derived from photographic interpretation undertaken by expert interpreters within the province of Ontario. Age is a common photo-interpreted attribute that we commonly see in forest resource inventories. However, forest age is often extremely difficult to estimate from either aerial or satellite imagery looking down. This has two implications for the analysis. First, given that we did utilize these photo-interpreted estimates of age, there are likely to be significant amounts of error, which are generally unknown, which makes it difficult to quantify the error associated with this analysis with respect to this attribute. Work is underway, for example, by Maltman et al. (2023) to estimate stand age from a combination of remote sensing data sets and ALS. However, these estimates carry errors simply due to our inability to derive age information solely from observations of canopy characteristics. As a result of all of the attributes utilized in this analysis, age is the one that is likely to carry the most significant error.

Succession dynamics in mid to late forest stages are the result of abiotic and biotic factors acting independently or interactively (Anyomi et al., 2022; Taylor and Chen, 2011). However, our analysis clearly demonstrates that there are key suite indicators that are useful for predicting species changes over time and space. Anyomi et al. (2022) described that boreal forests in Ontario exhibit long periods of compositional stability driven by strong successional inertia, punctuated by disturbance-induced pulses of change. Our findings align with these inertia-dominated successional dynamics, showing an overall low transition rate (~5%) but with identifiable transitions associated with mortality rates, structural attributes and insect activity. In this context, remotely sensed indicators function as early-warning indicators of emerging compositional shifts. Recent large-scale empirical analyses have shown that boreal successional transitions are highly nonlinear and driven by multiple interacting processes operating at different temporal and spatial scales, including species dominance, stand structure, gap dynamics, and disturbance history. For example, Zhu et al. (2025) used boosted regression trees and structural equation modeling across >3000 permanent plots and found that successional transitions occur with low probability (~4–5% per census interval) and are primarily driven by within-community dynamics such as species dominance and demographic structure rather than by any single external driver.

Although ALS data were available for a single acquisition year (2018), we interpret ALS-derived canopy structure as an integrated representation of cumulative stand development and gap legacy resulting from background mortality, competition, and non-stand-replacing disturbances. This framing is supported by recent work

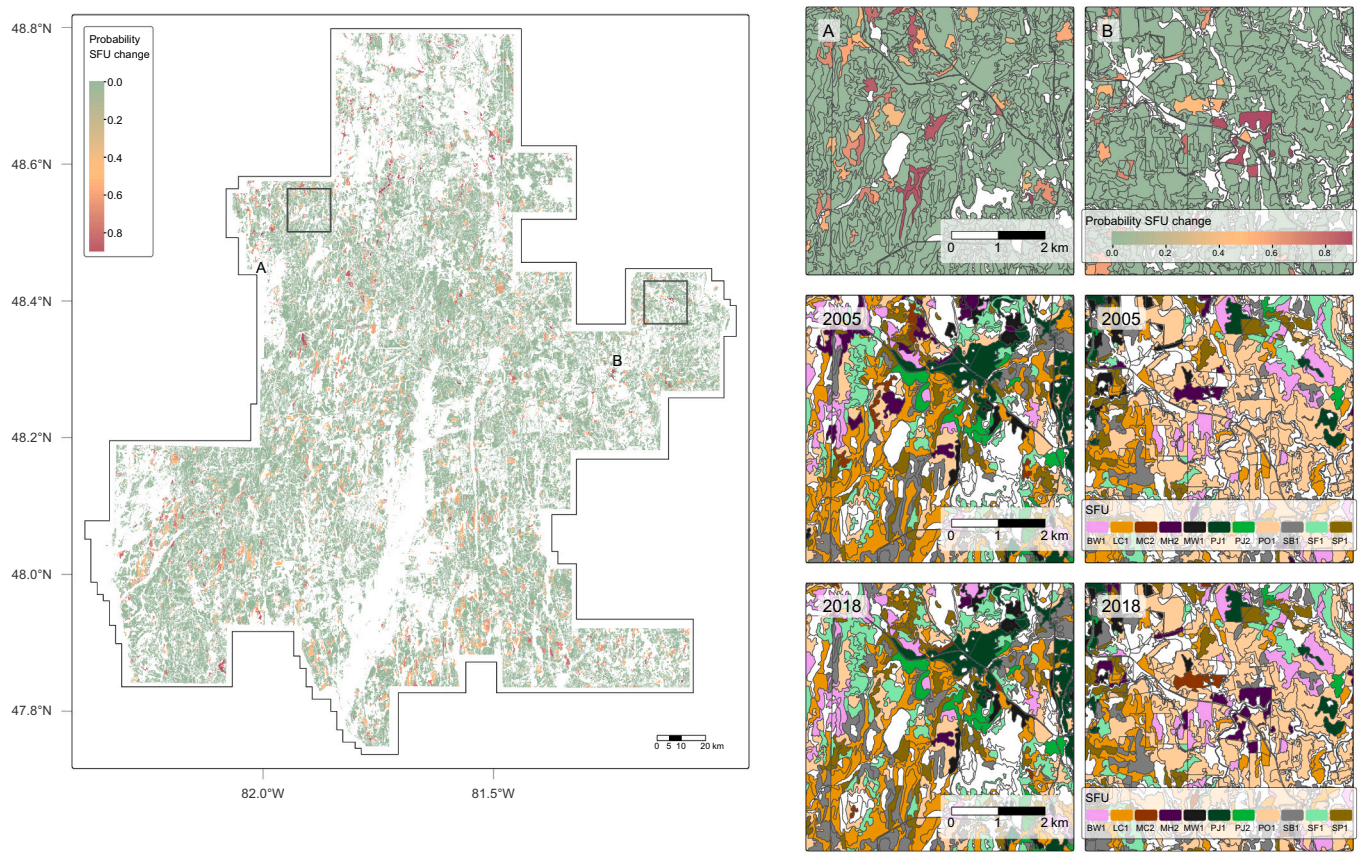

Fig. 5. Probability of species composition change at the stand level between 2005 and 2018 in the Romeo Mallette Forest area. Inset highlights the variation of the probability of species composition change at a finer spatial scale. SFU's abbreviations in Table 1.

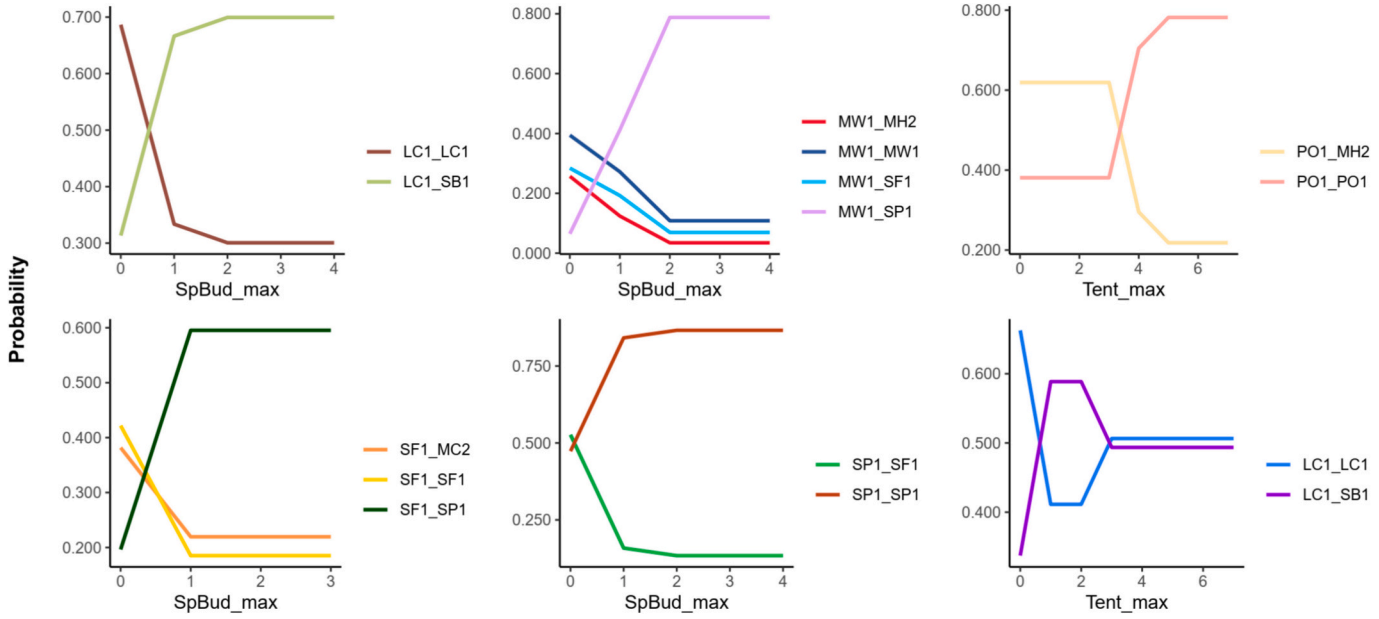

Fig. 6. Partial dependency plots showing the influence of the total number of years with defoliation events due to spruce budworm (SpBud_max) and Forest Tent Caterpillar (Tent_max) outbreaks on the probability of SFU transition classes. SFU's abbreviations in Table 1.

showing that canopy gap and structural attributes derived from ALS are related to time-averaged mortality rates and their spatial variability in boreal forests (Riofrío et al., 2025). In addition, Ma et al. (2023) demonstrated that tree mortality during multi-year droughts is regulated by tree height and neighborhood canopy structure, with higher structural complexity reducing mortality via shading and lower evaporative demand. Accordingly, ALS predictors in this study are used to characterize the structural context within which species-composition

transitions occurred, rather than to infer the precise timing of individual disturbance events. We acknowledge that repeated ALS acquisitions would improve detection of the timing and magnitude of structural change associated with specific disturbance events, representing an important direction for future monitoring. For instance, Trotto et al. (2024) demonstrated that the impact of repeated non-stand-replacing disturbances can manifest as structural changes detectable through ALS metrics such as canopy cover and height percentiles.

One of the critical variables that is often dominant in the variable importance is the gap area of the stand (derived from ALS data) and estimates of stand mortality rate (i.e., relative basal area loss). Analysis of gaps from ALS data is a well-established technique and one that is being utilized globally to better understand disturbance characteristics and growth patterns in forests worldwide (Jucker, 2022). Despite the relative high precision and flexibility of ALS data to detect and delineate canopy gaps, ALS datasets are rarely acquired at short intervals, which limits their operational use for routine monitoring forest canopy dynamics (Zhang et al., 2025). There have been a number of reviews examining different patterns of gap size distributions in forest types globally (Goodbody et al., 2020; Rodes-Blanco et al., 2023) and the application of these approaches to assess mortality also demonstrates the usefulness of this information for forest management activities (Huertas et al., 2022; Riofrío et al., 2025). One area of future work is the continued refinement and accuracy assessment of these gap detection techniques (Coops et al., 2021; Fischer et al., 2024). Field-based estimates of gaps are challenging to acquire and would ideally be directly measured within the forest stand. In reality, other remote sensing type techniques, for example, hemispherical photographs, are used to validate ALS estimates, but direct correlation of ALS-derived gaps with field measured gap area is challenging (Gaulton and Malthus, 2010). Given the importance of gaps in these mortality predictions and in helping explain the observed species shifts, validation of gap estimates and their application at fine spatial scales to inform management is a logical next direction.

Although our results showed that multiple pathways exist among SFUs, we found that stands dominated by black spruce and jack pine tend to be more stable than more diverse forests (low in species dominance), for example, mixed conifers, mixed hardwoods and mixedwoods types. Zhu et al. (2025) obtained similar findings, suggesting that forest dynamics like mortality, recruitment and growth are primary drivers of successional transitions on diverse stands, while disturbances and structural attributes highly drive transitions on forest dominated by a single species. For instance, the two most frequent transitions—MH2 to MC2 and SF1 to SP1—correspond well with known disturbance-mediated successional pathways. The former likely reflects localized FTC-related impacts on trembling aspen, while the latter is consistent with selective loss of balsam fir in SF1 stands where this species represents less than 35% of composition and is most susceptible to spruce budworm.

Our findings highlight the importance of disturbance regimes to define the likely successional pathway, especially in stands dominated by species more susceptible to spruce budworm or FTC defoliation events. The resulting patterns of FTC influencing hardwood-to-mixedwood transitions is consistent with well-established disturbance–succession theory and empirical studies of mixedwood dynamics (e.g., Moulinier et al., 2013). FTC infestation duration showed a weak but increasing effect on transition probability at higher defoliation intensities, particularly for stands with higher hardwood content. This pattern supports the hypothesis that FTC may contribute **to** PO1 to MH2 transitions in the eastern portion of the RMF. Similarly, Moulinier et al. (2013) reported that multiple years of defoliation likely caused more rapid canopy transition from aspen dominated to mixedwood stands. Authors noted that the proportion of large gaps and aspen mortality increased with FTC defoliation intensity that will likely accelerate the transition to mixedwood stands.

On the other hand, we observed a limited but detectable influence of spruce budworm in spruce–fir systems, for instance, stands are likely transitioning to a spruce-pine composition (SP1) after repeated cycles of defoliation and infestation. Because SBW activity during the study period was weak and RMF is dominated by black spruce (a relatively resistant host), any SBW-related compositional effects are expected to be modest and concentrated in minority host components. We therefore interpret SBW covariates as potential contributors to localized, small-magnitude shifts rather than as primary drivers of broad landscape-scale transitions. The different susceptibility among host species to spruce budworm triggers mortality (Bouchard and Pothier, 2010), provides stability (Sánchez-Pinillos et al., 2019) or reduces growth at different rates (Morin-Bernard et al., 2024), where typically, black spruce-dominated forests are usually less defoliated than balsam fir or white spruce forests (Hennigar et al., 2008). Moreover, initial canopy cover and stand height are key attributes that modulate the spruce budworm infestation severity, where more open stands are less susceptible to infestations (Trotto et al., 2024).

While the spatial variability of canopy cover, height and forest structural attributes can be accurately captured by ALS data, the current characterization of spruce budworm damage and delineation of infested area by periodic interpretation of aerial surveys may potentially provide limited temporal and spatial information on disturbance distribution, especially for light and intermediate attacks at a fine scale (Coops et al., 2020). The combination of aerial or satellite imagery with structural metrics derived from point clouds has shown promising results to provide fine spatial, spectral, and temporal scale analyses of forest insect disturbances (Rahimzadeh-Bajgiran et al., 2018; Senf et al., 2017; Trumbore et al., 2015). For instance, digital photogrammetric point clouds, derived using visible and near-infrared aerial imagery, might facilitate estimation of cumulative spruce budworm defoliation (Goodbody et al., 2018). Additionally, the availability of concurrent ALS acquisitions allows characterize the changes in structural attributes associated with different severity levels of spruce budworm attacks (Trotto et al., 2024).

Producing detailed spatial and multitemporal information of tree species requires non-trivial methodological considerations to ensure the consistency of the mapped species and that the observed changes in species composition represent the likely successional transitions. For instance, applying algorithms that consider the spatial and temporal differences of the spectral signature for a given species from multiple ecological zones, species assemblages, and environmental conditions (Fassnacht et al., 2016; Hermosilla et al., 2024; Gilić et al., 2023). However, national accuracy statistics of species classification cannot be directly assumed at local-scale (i.e., RMF), because the occurrence probability of non-dominant species may not necessarily reflect their prevalence in a given pixel. Thus a careful consideration of thresholds are required to determine their meaningful presence (Hermosilla et al., 2022). Beside defining thresholds for class membership at pixel level and the relative presence per stand for a given species, a local validation of species classification is advised to assess the discrepancies between model predictions and reference species composition. In our local validation, Landsat-derived SFU classification achieve local accuracies >60% for most SFU classes in comparison to FRI photo-interpreted SFU (Fig. S1). It is worth to note that SFU misclassification were systematic, not random, and primarily restricted to SFU classes with similar species compositions, such as, spruce–fir vs. spruce–pine (SF1–SP1), birch-poplar vs. mixed hardwood (BW1–MH2) and mixed conifers (MC2). The accuracy levels in our validation assessment are comparable to recent studies combining multispectral imagery and ALS data to estimate species proportions at stand level. For example, Cao et al. (2025) and Murray et al. (2025) achieved species prediction errors on the order of 10–20% depending on the taxon and stand composition. Although these approaches estimate continuous species proportions rather than discrete SFU classes, their reported uncertainty ranges align with the accuracy levels we observe locally and reinforce that our detected transitions are unlikely to result from random misclassification.

Moreover, considering established successional transition rules (Lennon et al., 2016) and the temporal consistency assessment of SFU transitions might help to refine the time series and reduce the uncertainty related to the species mapping (Gómez et al., 2016), especially for developing local applications that facilitate informed decisions regarding forest management and conservation planning.

The implementation of a continuous forest inventory framework (Coops et al., 2023; Mulverhill et al., 2024) to deliver updated forest inventory attributes cost-effectively also requires updated information on forest composition. Together, the Landsat-based species composition trajectories and structural attributes and mortality estimates derived from ALS data represent a set of ecological indicators that capture both compositional and structural dimensions of forest condition. These indicators respond to disturbance gradients, revealing the magnitude and direction of successional shifts, and can be consistently mapped across management units. Moreover, flagging stands that are likely to show changes in species composition would facilitate an effective method for designing a field measurement program to validate the forest inventory outcomes. Lastly, managers can leverage from accurate, spatially explicit, and detailed information to design and implement adaptative silviculture regimes at for operational management scale (Achim et al., 2022), especially with more frequent and drastic disturbances to be expected.

5. Conclusion

This study illustrates the value of integrating satellite-derived species composition time series, ALS-based structural attributes and disturbance history to detect and predict species composition transitions in boreal mixedwood forests. This integration enabled us to identify and model 27 compositional transitions within mid to late successional stages. While only a small fraction of the landscape experienced species composition changes within the 13-year study window, these changes were strongly associated with mortality rates and canopy gaps. Additionally, stands with repeated defoliation from spruce budworm outbreaks exhibited higher probabilities of transition, particularly to spruce-pine assemblages. These results underscore the importance of structural and disturbance-based indicators in understanding and forecasting species shifts during mid to late successional stages. The relatively low overall area undergoing transition reflects both the slow pace of forest succession and the short temporal window considered. By identifying stands prone to compositional change, our findings support the development of continuous forest inventory systems and inform adaptive silvicultural planning to enhance resilience under increasing disturbance pressures. Moreover, combining Landsat-derived species-assemblage trajectories with ALS-derived structural and mortality metrics, our analysis provides a suite of spatially explicit indicators relevant for assessing forest integrity and monitoring successional dynamics across managed boreal landscapes.

CRediT authorship contribution statement

José Riofrío: Writing – review & editing, Writing – original draft, Visualization, Validation, Software, Methodology, Investigation, Formal analysis, Data curation, Conceptualization. **Nicholas C. Coops:** Writing – review & editing, Writing – original draft, Supervision, Resources, Project administration, Methodology, Funding acquisition, Conceptualization. **Muhammad Waseem Ashiq:** Writing – review & editing, Methodology, Conceptualization. **Alexis Achim:** Writing – review & editing, Supervision, Resources, Project administration, Methodology, Funding acquisition, Conceptualization.

Declaration of competing interest

The authors declare that they have no known competing financial interests or personal relationships that could have appeared to influence the work reported in this paper.

Acknowledgments

This work was supported by the NSERC Alliance Grant Project Silva21 [NSERC ALLRP 556265-20]. We thank the Ontario Ministry of Natural Resources for sharing the SPL data as well as the permanent sample plot data collected at the Romeo Mallette Forest. We would also like to thank GreenFirst Forest Products for accessing the polygon inventory data required for this study.

Appendix A. Supplementary data

Supplementary data to this article can be found online at https://doi.org/10.1016/j.ecolind.2026.114659.

Data availability

Annual tree species maps data is available at https://opendata.nfis.org/mapserver/nfis-change_eng.html. Airborne laser scanning and permanent sample plot data are available upon request from the Ontario Ministry of Natural Resources. Georeferenced layers of mapped events of forest insect damage are available online at https://geohub.lio.gov.on.ca/.

References

Achim, A., Moreau, G., Coops, N.C., Axelson, J.N., Barrette, J., Bédard, S., Byrne, K.E., Caspersen, J., Dick, A.R., D'Orangeville, L., Drolet, G., Eskelson, B.N.I., Filipescu, C. N., Flamand-Hubert, M., Goodbody, T.R.H., Griess, V.C., Hagerman, S.M., Keys, K., Lafleur, B., Girona, M.M., Morris, D.M., Nock, C.A., Pinno, B.D., Raymond, P., Roy, V., Schneider, R., Soucy, M., Stewart, B., Sylvain, J.D., Taylor, A.R., Thiffault, E., Thiffault, N., Vepakomma, U., White, J.C., 2022. The changing culture of silviculture. Forestry 95, 143–152.

Anyomi, K.A., Neary, B., Chen, J., Mayor, S.J., 2022. A critical review of successional dynamics in boreal forests of North America. Environ. Rev. 30, 563–594.

Bergeron, Y., Chen, H.Y.H., Kenkel, N.C., Leduc, A.L., Macdonald, S.E., 2014. Boreal mixedwood stand dynamics: ecological processes underlying multiple pathways. For. Chron. 90, 202–213.

Bonannella, C., Parente, L., De Bruin, S., Herold, M., 2024. Multi-decadal trend analysis and forest disturbance assessment of European tree species: concerning signs of a subtle shift. For. Ecol. Manage. 554, 121652.

Bouchard, M., Pothier, D., 2010. Spatiotemporal variability in tree and stand mortality caused by spruce budworm outbreaks in eastern Quebec. Can. J. For. Res. 40, 86–94.

Brassard, B.W., Chen, H.Y.H., 2010. Stand structure and composition dynamics of boreal mixedwood forest : implications for forest management. Sustain. For. Manage. Network 19.

Cao, Y., Coops, N.C., Murray, B.A., Sinclair, I., 2025. Enhancing tree species composition mapping using Sentinel-2 and multi-seasonal deep learning fusion. Int. J. Remote Sens. 0, 1–27.

Caspersen, J.P., 2004. Variation in stand mortality related to successional composition. For. Ecol. Manage. 200, 149–160.

Chen, H.Y.H., Popadiouk, R.V., 2002. Dynamics of North American boreal mixedwoods. Environ. Rev. 10, 137–166.

Chen, T., Guestrin, C., 2016. XGBoost: A scalable tree boosting system. In: Proceedings of the 22nd ACM SIGKDD International Conference on Knowledge Discovery and Data Mining. Presented at the KDD '16: The 22nd ACM SIGKDD International Conference on Knowledge Discovery and Data Mining, ACM, San Francisco California USA, pp. 785–794.

Coops, N.C., Shang, C., Wulder, M.A., White, J.C., Hermosilla, T., 2020. Change in forest condition: characterizing non-stand replacing disturbances using time series satellite imagery. For. Ecol. Manage. 474, 118370.

Coops, N.C., Tompalski, P., Goodbody, T.R.H., Queinnec, M., Luther, J.E., Bolton, D.K., White, J.C., Wulder, M.A., van Lier, O.R., Hermosilla, T., 2021. Modelling lidar-derived estimates of forest attributes over space and time: a review of approaches and future trends. Remote Sens. Environ. 260, 112477.

Coops, N.C., Tompalski, P., Goodbody, T.R.H., Achim, A., Mulverhill, C., 2023. Framework for near real-time forest inventory using multi source remote sensing data. Forestry: Int. J. For. Res. 96, 1–19.

Fassnacht, F.E., Latifi, H., Stereńczak, K., Modzelewska, A., Lefsky, M., Waser, L.T., Straub, C., Ghosh, A., 2016. Review of studies on tree species classification from remotely sensed data. Remote Sens. Environ. 186, 64–87.

Fassnacht, F.E., White, J.C., Wulder, M.A., Næsset, E., 2024. Remote sensing in forestry : current challenges, considerations and directions. Forestry: Int. J. For. Res. 97, 11–37.

Fenton, N.J., Bergeron, Y., 2013. Stochastic processes dominate during boreal bryophyte community assembly. Ecology 94, 1993–2006.

Ferri, C., Hernández-Orallo, J., Modroiu, R., 2009. An experimental comparison of performance measures for classification. Pattern Recogn. Lett. 30, 27–38.
Fischer, F.J., Jackson, T., Vincent, G., Jucker, T., 2024. Robust characterisation of forest structure from airborne laser scanning—a systematic assessment and sample workflow for ecologists. Meth. Ecol. Evol. 15, 1873–1888.
Friedman, J.H., 2001. Greedy function approximation: a gradient boosting machine. Ann. Stat. 29, 1189–1232.
Friedman, J.H., Meulman, J.J., 2003. Multiple additive regression trees with application in epidemiology. Stat. Med. 22, 1365–1381.
Gaulton, R., Malthus, T.J., 2010. LiDAR mapping of canopy gaps in continuous cover forests: a comparison of canopy height model and point cloud based techniques. Int. J. Remote Sensing 31, 1193–1211.
Gilić, F., Gašparović, M., Baučić, M., 2023. Current state and challenges in producing large-scale land cover maps: review based on recent land cover products. Geocarto Int. 38, 2242693.
Gillis, M.D., Omule, A.Y., Brierley, T., 2005. Monitoring Canada's forests: the National Forest Inventory. For. Chron. 81, 214–221.
Gluckman, J., 2016. Design of the Processing Chain for a High-Altitude, Airborne, Single-Photon Lidar Mapping Instrument. Laser Radar Technology and Applications XXI, In, pp. 20–28.
Gómez, C., White, J.C., Wulder, M.A., 2016. Optical remotely sensed time series data for land cover classification: a review. ISPRS J. Photogramm. Remote Sens. 116, 55–72.
Goodbody, T.R.H., Coops, N.C., Hermosilla, T., Tompalski, P., McCartney, G., MacLean, D.A., 2018. Digital aerial photogrammetry for assessing cumulative spruce budworm defoliation and enhancing forest inventories at a landscape-level. ISPRS J. Photogrammetry Remote Sensing 142, 1–11.
Goodbody, T.R.H., Tompalski, P., Coops, N.C., White, J.C., Wulder, M.A., Sanelli, M., 2020. Uncovering spatial and ecological variability in gap size frequency distributions in the Canadian boreal forest. Sci. Rep. 10, 1–12.
Greenwell, B., M., 2017. Pdp: an R package for constructing partial dependence plots. The R Journal 9, 421.
Greenwell, B., Boehmke, B., Cunningham, J., Developers, G., Greenwell, M.B., 2019. Package 'gbm.' R package version 2.
Hart, J.L., Kleinman, J.S., 2018. What are intermediate-severity forest disturbances and why are they important? Forests 9.
Hastie, T., Tibshirani, S., Friedman, H., 2009. The Elements of Stattistical Learning: Data Mining, Inference, and Prediction, Second edition. ed. Springer. Springer Series in Statistics.
Hennigar, C.R., MacLean, D.A., Quiring, D.T., Kershaw, J.A., 2008. Differences in spruce budworm defoliation among balsam fir and White, red, and black spruce. For. Sci. 54, 158–166.
Hermosilla, T., Bastyr, A., Coops, N.C., White, J.C., Wulder, M.A., 2022. Mapping the presence and distribution of tree species in Canada's forested ecosystems. Remote Sens. Environ. 282, 113276.
Hermosilla, T., Wulder, M.A., White, J.C., Coops, N.C., Bater, C.W., Hobart, G.W., 2024. Characterizing long-term tree species dynamics in Canada's forested ecosystems using annual time series remote sensing data. For. Ecol. Manage. 572, 122313.
Huertas, C., Sabatier, D., Derroire, G., Ferry, B., Jackson, T.D., Pelissier, R., Vincent, G., 2022. Mapping tree mortality rate in a tropical moist forest using multi-temporal LiDAR. Int. J. Appl. Earth Obs. Geoinf. 109.
Jucker, T., 2022. Deciphering the fingerprint of disturbance on the three-dimensional structure of the world's forests. New Phytol. 233, 612–617.
Kuhn, M., 2015. Caret: classification and regression training. Astrophysics Source Code Library ascl-1505.
Lennon, K., Parton, J., Major, K., Kayahara, G.J., 2016. Evidence-Based Natural Succession Pathways for Forest Management Planning in Northeastern Ontario (Technical Report No. TR-15).. Ministry of Natural Resources and Forestry, Science and Research Branch, Peterborough, ON.
Little, T.I., Kayahara, Gordon J., Russell, L.A., Nsiah, Samuel K., Vasiliauskas, Stan, 2024. Standard Forest Units for the Northeast Boreal Forest Region in Ontario, second edition (vols. No. TM-12. Science and Research Technical Manual. Ontario Ministry of Natural Resources, Peterborough, ON.
Liu, Z., Yang, J., 2014. Quantifying ecological drivers of ecosystem productivity of the early-successional boreal Larix gmelinii forest. Ecosphere 5, art84.
Ma, Q., Su, Y., Niu, C., Ma, Q., Hu, T., Luo, X., Tai, X., Qiu, T., Zhang, Y., Bales, R.C., Liu, L., Kelly, M., Guo, Q., 2023. Tree mortality during long-term droughts is lower in structurally complex forest stands. Nat. Commun. 14.
Maltman, J.C., Hermosilla, T., Wulder, M.A., Coops, N.C., White, J.C., 2023. Estimating and mapping forest age across Canada's forested ecosystems. Remote Sens. Environ. 290, 113529.
McCarthy, J., 2001. Gap dynamics of forest trees: a review with particular attention to boreal forests. Environ. Rev. 9, 1–59.
MNR, 2024. Forest Insect Damage Event.
Morin-Bernard, A., Achim, A., Coops, N.C., White, J.C., 2024. Integration of tree-ring data, Landsat time series, and ALS-derived topographic variables to quantify growth declines in black spruce. For. Ecol. Manage. 557, 121765.
Moulinier, J., Lorenzetti, F., Bergeron, Y., 2013. Effects of a forest tent caterpillar outbreak on the dynamics of mixedwood boreal forests of eastern Canada. Écoscience 20, 182–193.
Mulverhill, C., Coops, N.C., White, J.C., Tompalski, P., Achim, A., 2024. Evaluating the potential for continuous update of enhanced forest inventory attributes using optical satellite data. Forestry: Int. J. For. Res. 98, 253–265.
Murray, B.A., Coops, N.C., White, J.C., Dick, A., Ragab, A., 2025. Tree species proportion prediction using airborne laser scanning and Sentinel-2 data within a deep learning based dual-stream data fusion approach. Int. J. Remote Sens. 46, 5436–5464.
Nakadai, R., Suzuki, S.N., 2025. Ecological succession revisited from a temporal beta-diversity perspective. For. Ecol. Manage. 580, 122504.
Natekin, A., Knoll, A., 2013. Gradient Boosting Machines, a Tutorial. Front, Neurorobot, p. 7.
National Forestry Database, 2025. Forest Insects: Spruce Budworm, 1990–2022.
Ontario Ministry of Natural Resources, 2009. Forest Resources Inventory Technical Specifications. Ontario Ministry of Natural Resources.
Ontario Ministry of Natural Resources, 2016. Ontario Specifications for Lidar Acquisition (No. Version 1.1 (2016-05-09)). Ontario Ministry of Natural Resources.
Ontario Ministry of Natural Resources, 2018. 2019–2029 Forest Management Plan - Analysis Package for the Romeo Malette Forest. Ontario Ministry of Natural Resources, Timmins.
Ontario Ministry of Natural Resources, 2021. Vegetation sampling network protocol: Technical specifications for field plots (no. TM-10), Science and Research Technical Manual. Ontario Ministry of Natural Resources, Science and Research Branch, Peterborough, ON.
Parton, J., Vasiliauskas, S., Lucking, G., Watt, W.R., 2006. Standard Forest Units for Northeastern Ontario Boreal Forests. OMNR, Northeast Science & Information, NESI Technical Note TN-021.
Patton, D.R., 1975. A diversity index for quantifying habitat " edge ". Wildl. Soc. Bull. 3, 171–173.
Penner, M., Pitt, D., 2019. The Ontario Growth and Yield Program Status and Needs – Report to the Forestry Futures Trust Committee.
Poorter, L., van der Sande, M.T., Amissah, L., Bongers, F., Hordijk, I., Kok, J., Laurance, S.G.W., Martínez-Ramos, M., Matsuo, T., Meave, J.A., Muñoz, R., Peña-Claros, M., van Breugel, M., Herault, B., Jakovac, C.C., Lebrija-Trejos, E., Norden, N., Lohbeck, M., 2024. A comprehensive framework for vegetation succession. Ecosphere 15.
Rahimzadeh-Bajgiran, P., Weiskittel, A.R., Kneeshaw, D., MacLean, D.A., 2018. Detection of annual spruce budworm defoliation and severity classification using Landsat imagery. Forests 9, 357.
Rees, M., Condit, R., Crawley, M., Pacala, S., Tilman, D., 2001. Long-term studies of vegetation dynamics. Science 293, 650–655.
Riofrío, J., Coops, N.C., Ashiq, M.W., Achim, A., 2025. Mapping mortality rates in boreal mixedwood forest using airborne laser scanning and permanent plot data. Forestry: Int. J. For. Res. cpaf002.
Rodes-Blanco, M., Ruiz-Benito, P., Silva, C.A., García, M., 2023. Canopy gap patterns in Mediterranean forests: a spatio-temporal characterization using airborne LiDAR data. Landsc. Ecol. 38, 3427–3442.
Roussel, J.R., Auty, D., Coops, N.C., Tompalski, P., Goodbody, T.R.H., Meador, A.S., Bourdon, J.F., de Boissieu, F., Achim, A., 2020. lidR: an R package for analysis of airborne laser scanning (ALS) data. Remote Sens. Environ. 251, 112061.
Sales, M.H.R., de Bruin, S., Souza, C., Herold, M., 2022. Land use and land cover area estimates from class membership probability of a random Forest classification. IEEE Trans. Geosci. Remote Sens. 60, 1–11.
Sánchez-Pinillos, M., Leduc, A., Ameztegui, A., Kneeshaw, D., Lloret, F., Coll, L., 2019. Resistance, resilience or change: post-disturbance dynamics of boreal forests after insect outbreaks. Ecosystems 22, 1886–1901.
Senf, C., Seidl, R., Hostert, P., 2017. Remote sensing of forest insect disturbances: current state and future directions. International Journal of Applied Earth Observation and Geoinformation 60, 49–60.
Silva, C.A., Valbuena, R., Pinagé, E.R., Mohan, M., de Almeida, D.R.A., North Broadbent, E., Jaafar, W.S.W.M., de Almeida Papa, D., Cardil, A., Klauberg, C., 2019. ForestGapR: an r package for forest gap analysis from canopy height models. Methods Ecol. Evol. 10, 1347–1356.
Taylor, A.R., Chen, H.Y.H., 2011. Multiple successional pathways of boreal forest stands in Central Canada. Ecography 34, 208–219.
Taylor, A.R., Endicott, S., Hennigar, C., 2020. Disentangling mechanisms of early succession following harvest: implications for climate change adaptation in Canada's boreal-temperate forests. For. Ecol. Manage. 461, 117926.
Trotto, T., Coops, N.C., Achim, A., Gergel, S.E., Roeser, D., 2024. Characterizing forest structural changes in response to non-stand replacing disturbances using bitemporal airborne laser scanning data. Science of Remote Sensing 10, 100160.
Trumbore, S., Brando, P., Hartmann, H., 2015. Forest health and global change. Science 349, 814–818.
Vidal-Macua, J.J., Ninyerola, M., Zabala, A., Domingo-Marimon, C., Pons, X., 2017. Factors affecting forest dynamics in the Iberian Peninsula from 1987 to 2012. The role of topography and drought. For. Ecol. Manage. 406, 290–306.
White, J.C., Tompalski, P., Vastaranta, M., Wulder, M.A., Stepper, C., Ninni, S., Coops, N. C., 2017. A Model Development and Application Guide for Generating an Enhanced Forest Inventory Using Airborne Laser Scanning Data and an Area-Based Approach. Natural resources Canada, Victoria, Canada.
White, J.C., Tompalski, P., Coops, N.C., Wulder, M.A., 2018. Comparison of airborne laser scanning and digital stereo imagery for characterizing forest canopy gaps in coastal temperate rainforests. Remote Sens. Environ. 208, 1–14.
White, J.C., Tompalski, P., Bater, C.W., Wulder, M.A., Fortin, M., Hennigar, C., Robere-McGugan, G., Sinclair, I., White, R., 2025. Enhanced forest inventories in Canada: implementation, status, and research needs. Can. J. For. Res. 55, 1–37.
Wulder, M.A., Hermosilla, T., White, J.C., Bater, C.W., Hobart, G., Bronson, S.C., 2024. Development and implementation of a stand-level satellite-based forest inventory for Canada. Forestry: Int. J. For. Res. 97, 546–563.

Yamamoto, S.-I., 2000. Forest gap dynamics and tree regeneration. J. For. Res. 5, 223–229.
Zhang, B., Jackson, T.D., Coomes, D.A., Burslem, D.F.R.P., Nilus, R., Bittencourt, P.R.L., Bartholomew, D.C., Rowland, L., Fischer, F.J., Jucker, T., 2025. Soils and topography drive large and predictable shifts in canopy dynamics across tropical forest landscapes. New Phytol. 247, 1666–1679.
Zhu, Y., Chen, J., Ashiq, M.W., Chen, H.Y.H., Mayor, S., 2025. Complex ecological pathways drive boreal forest successional dynamics. For. Ecol. Manage. 590, 122820.